



PHOTOLUMINESCENCE FROM GaAs NANOSTRUCTURES

By

Alemu Gurmessa Gindaba

SUBMITTED IN PARTIAL FULFILLMENT OF
THE REQUIREMENTS FOR THE DEGREE OF
MASTER OF SCIENCE IN PHYSICS
(CONDENSED MATTER PHYSICS)

AT

JIMMA UNIVERSITY
JIMMA, ETHIOPIA

JUNE 2014

JIMMA UNIVERSITY
COLLEGE OF NATURAL SCIENCE
DEPARTMENT OF PHYSICS

Supervisor:

1. Prof. L.V Choudary
2. Mr. Getnet Melese

External Examiner:

Dr. Chernet Amente

Internal Examiner

Dr. Sisay Shewamare

JIMMA UNIVERSITY

Date: **June 2014**

Author: **Alemu Gurmessa Gindaba**

Title: **PHOTOLUMINESCENCE FROM GaAs
NANOSTRUCTURES**

Department: **Physics**

Degree: **M.Sc.** Convocation: **June** Year: **2014**

Permission is herewith granted to Jimma University to circulate and to have copied for non-commercial purposes, at its discretion, the above title upon the request of individuals or institutions.

Signature of Author

THE AUTHOR RESERVES OTHER PUBLICATION RIGHTS, AND NEITHER THE THESIS NOR EXTENSIVE EXTRACTS FROM IT MAY BE PRINTED OR OTHERWISE REPRODUCED WITHOUT THE AUTHOR'S WRITTEN PERMISSION.

THE AUTHOR ATTESTS THAT PERMISSION HAS BEEN OBTAINED FOR THE USE OF ANY COPYRIGHTED MATERIAL APPEARING IN THIS THESIS (OTHER THAN BRIEF EXCERPTS REQUIRING ONLY PROPER ACKNOWLEDGEMENT IN SCHOLARLY WRITING) AND THAT ALL SUCH USE IS CLEARLY ACKNOWLEDGED.

Haadha manaa kootiif

Table of Contents

Table of Contents	vi
List of Figures	vii
Abstract	x
Acknowledgements	xi
1 Introduction	1
2 Theoretical background of the study	4
2.1 Semiconductor materials	4
2.1.1 Fabrication of Semiconductor AlGaAs/GaAs Nanostructure	6
2.1.2 Application of AlGaAs/GaAs semiconductor nanostructure	7
2.2 Quantum confinement and optical properties	8
2.2.1 Quantum Dots	8
2.2.2 Quantum wires	9
2.2.3 Quantum Wells.	10
2.3 Density of states	11
2.3.1 Density of states Bulk	11
2.3.2 Density of States of Quantum Well,Quantum wires and Quantum dots	13
2.3.3 Population of the conduction band	16
2.3.4 Fermi Level	18
2.4 Dynamics of charge carriers in semiconductors nanostructures	19
2.4.1 Radiative recombination	21
2.4.2 Nonradiative recombination	21
2.4.3 Excitons	22
2.5 Photoluminescence	24
2.6 Analytical Calculation of optical parameters on photoluminescence intensity	26
2.6.1 Temperature dependence of PL emission	26
2.6.2 Optical Absorption and emission	27
2.6.3 The quantum confinement model (QCM)	28

2.6.4	Time Resolved	31
3	Methodology	33
3.1	Analytical method	34
3.2	Numerical method	34
4	Result and discussion	35
4.1	PL Intensity vs Temperature	35
4.2	PL Intensity vs Wavelength	37
4.3	PL Intensity Vs size	38
4.4	PL Intensity Vs Photon energy	39
4.5	PL Intensity Vs Time	39
5	Conclusion and future outlooks	42
5.1	Conclusion	42
5.2	Future Outlook	43
	Bibliography	44

List of Figures

2.1	Direct band transition	5
2.2	Indirect band transition	6
2.3	Band structure of Gallium arsenide (GaAs)	8
2.4	Constant-energy spherical surfaces in k-space	11
2.5	Constant-energy perimeters in k-space. the (x, y) plane.	13
2.6	Reduction of the dimensionality of semiconductor system from 3D to 0D	16
2.7	(Generation, Relaxation and Recombination.)	20
2.8	(a-c) Radiative recombination paths: (a) band-to band; (b) donor to valence band; (c) conduction band to acceptor. (d) Nonradiative recombination via an intermediate state.	20
2.9	Exciton of electron-hole.	22
2.10	Processes involved in a photoluminescence experiment. The non-resonant photons are absorbed, creating hot electrons and holes	25
2.11	schematically diagram depict Size dependent of PL in (from left to right size decreasing blue shift spectrum)	26
4.1	PL intensity Vs photon energy matlab simulation result	35
4.2	PL transient measured at different wavelengths corresponding to the sizes of the GaAs QDs (a) simulation result.(b) taken from reference[19]	37
4.3	PL intensity versus size of the quantum cluster The simulation result when ($\delta = 0.003$ and 0.004)	38
4.4	PL intensity versus size of the quantum cluster simulation result $\delta = 0.003$ and 0.0004	39
4.5	PL intensity Vs photon energy (a) simulation result and (b) taken from reference [28]	40

4.6 PL intensity vs decay time*100ns (a) Diagram that shown the result of
matlab simulation and (b) Taken from reference[19] 41

Abstract

The confinement properties of semiconductor nanostructures has promising potential in technological application. Such application originated from the features confined nanostructures, that could be analysed through a mechanism PL spectroscopy which probed different properties of materials. The main objective of this study is to describe the dependence of PL intensity on optical parameters temperature, time decay, absorption and emission (wavelength) and photon energy semiconductor nanostructures of unstrained and intrinsic GaAs quantum dots. The theoretical and practical model equations were numerically analyzed and simulated with matlab and fortran 90 codes to draw an agreement with supposed theoretical and experimental values. The experimental fitted values and physical properties of materials were used as data source for our simulation. We reached with conclusion at low temperature the peak is quite sharp, as temperature increases we observed the PL intensity decreased and got quenched at particular thermal energy. As photon energy increases the peak broadens shifts to the lower energy. As the wavelength increases PL intensity decrease. At the mean value diameter 10nm PL intensity reach peaks while the diameter increases exceeding mean value of diameter PL intensity decreases. Such that our simulation result made agreement with theoretical supposition.

Acknowledgements

First and foremost I would like to thank the Almighty GOD, With his mercy and help I could accomplished this thesis work.

I would like to express my grateful, gratitude and sincere appreciation to my advisors, Prof, L.V Choudary and Mr.Getnet Melese for their guidance, valuable advice and consistent support at all the stage of this thesis work.

I want also to express my deep appreciation to Mr Seid Mohammed, Mr.Gemechu Mul'ata and my friend Alemayehu Keno for any academic and technical support while I was conducting this thesis.

I would like to express the deepest and gratitude thank to my wife Habtame Beyene and my children Abene'ezer and Nataye Alemu without their patience, moral and financial support this work could not be accomplished.

My thanks also goes to all Jimma University Physics Department staff members (Mr.Gelana Chibsa head of department, Dr.Sisay Shawamare, Mr.Tolu Birssa, Mr.Hiwot Digafe, Prof.Vegi, Mr.Chali Yadeta, Mr.Solomon H/Mariam, Ms Hiwot,) for their professional support whenever and where ever required.

I would like to thank my uncle Teshome Abebe for he had laid foundation that determine the destine in all status of my life and academic carrier.

Lastly but not least I thank Jimma College of Teachers Education and Oromia Educational Bureau for sponsorship to attain this program

Chapter 1

Introduction

Nanostructure can be defined as a structure with size smaller than one hundred nanometer in at least one of the three dimensions, with a variety from two to zero dimension confinements, i.e. quantum well quantum wire and quantum dot. The study of PL intensity in other way side enable as to describe novel characteristic of semiconductor nanostructures with application of Photoluminescence PL, which is a very efficient, non-destructive, contactless and standard technique used to characterize and evaluate quality of surfaces and interfaces as well as to probe defect levels within the material [1]. The electronic properties of structures depend on the dimensionality and the geometric details of the materials [2]. Nanomaterials are the cornerstones of nanoscience and nanotechnology and are anticipated to play an important role in future economy, technology, and human life in general. The strong interests in nanomaterials stem from their unique physical and chemical properties and functionalities that often differ significantly from their corresponding bulk counterparts. Exceptionally large surface area to volume ratios relative to that the bulk produce variations in surface state populations that have numerous consequences on material properties [3].

The small size of nanostructures permits the infamous electronic device scaling for faster operation, lower cost and reduced power consumption. These unique properties have enabled the variety of electronic, photonic, and optoelectronic information storage, communication, energy conversion, catalysis, environmental protection, and space exploration

applications based on semiconductor nanostructures [4]. Semiconductor nanoparticles, generally considered to be particles of material with diameters in the range of 1 to 10 nm [5]. This leads to the surface playing an important role in the properties of the material. The second factor is the actual size of the particle, there is a change in the electronic properties of the material; as the size of the solidities becomes smaller the band gap gradually becomes larger because of quantum confinement effects.

This effect is a consequence of the confinement of an "electron in a box" giving rise to discrete energy levels, rather than a continuous band as in the corresponding bulk material. Thus, for a semiconductor nanoparticle the "electron and hole" produced by the absorption of a photon are closer together than in the macro crystalline material, and as such the Columbic interaction cannot be neglected; they have higher kinetic energy than in the macrocrystalline material.

Consequently, the first excitonic transition (band gap) increases in energy with decreasing particle diameter GaAs is a ubiquitous semiconductor in both scientific studies and in the semiconductors industry for several researches. GaAs has exceptionally large Bohr excitation diameter 22.4nm relative to other semiconductor allowing for the case of experimental access to this fundamentally important threshold, similarly its high electron mobility $8500\text{cm}^2/\text{s}$ at room temperature is of the interest for electronic studies. GaAs forms nearly strain free alloy with AlAs(0.13) lattice mismatch [6] Quantum dots and optoelectronics. III-V compound semiconductor quantum dots (QDs) have gained scientific attention due to their potential utility as optoelectronic devices such as laser devices, photodetectors, and optical communication devices, Especially, GaAs-based optical devices have been of great interest since they can be used for opticalfiber- based communication systems at infrared wavelengths [7]. GaAs has some advantages in electronic properties which are superior to those of silicon. It has a higher saturated electron velocity and higher electron mobility, allowing transistors made from it to function at frequencies in excess of 250GHz . Unlike silicon junctions, GaAs devices are relatively insensitive to

heat owing to their wider band gap. Also, GaAs devices tend to have less noise than silicon devices especially at high frequencies which are a result of higher carrier mobilities and lower resistive device. These properties recommend GaAs circuitry in mobile phones, satellite communications, microwave point-to-point links and higher frequency radar systems.

It is used in the manufacture of Gun diodes for generation of microwaves. Another advantage of GaAs is that it has a direct band gap, that it can be used to emit light efficiently. While Silicon has an indirect band gap and so is very poor at emitting light. Nonetheless, recent advances may make silicon LEDs and lasers possible. As a wide direct band gap material and resulting resistance to radiation damage, GaAs is an excellent material for space electronics and optical windows in high power applications. Because of its wide band gap pure GaAs is highly resistive. Combined with the high dielectric constant, this property makes GaAs a very good electrical substrate and unlike Si provides natural isolation between devices and circuits [8]. In this study we address optical and electrical properties due to electron excitation from occupied Valence band to unoccupied conduction band in InGaAs/GaAs semiconductor nanostructures.

The study was focused dependence of PL intensity on parameters such photon energy, wavelength, temperature and size of the nanoclusters.

The main purpose this research contributes for the advancement of Nanoscience and Nanotechnology. Thus the nanostructure developed highly in group III-V elements and will provide good opportunity on knowledge and application for the researcher and other who will be interested to do more investigation on nanostructure [9]. It addressed the optical and electrical properties of semiconductors, dependence of photoluminescence intensity of InGaAs/ GaAs quantum dot on different parameters like photon energy, wavelength, bandgap, temperature and size of the nanoclusters.

Chapter 2

Theoretical background of the study

2.1 Semiconductor materials

The semiconductor nanoparticles have properties between molecules and bulk solid semiconductors. Their physicochemical properties are found to be strongly size dependent. It is well known that the nanoscale systems show interesting physical properties such as increasing semiconductor band gap due to electron confinement [10]. Semiconductor materials are classified into elemental (Group IV) and compound (group III-V) Semiconductor materials can be also classified into two in such direct band transition and indirect band transition. Quantum dots are nanometer-sized clusters of semiconductor material which confine electrons in all three directions. The physics of quantum dots are dominated by quantization : there are discrete energy levels, as in real atoms. Quantum dots can now be self-assembled directly in the growth of inorganic semiconductors, and this discovery has fueled an explosion in the interest in this field [11]. PL Intensity in Intrinsic/ undoped GaAs Quantum Dots was seen under different optical parameters such as temperature, size , time resolved, and wavelength got reviewed in this chapter in detail. GaAs is very resistant to radiation damage. This, along with its high efficiency makes GaAs very desirable for outer space applications. Thus, QDs are also referred to as superatoms or artificial atoms [2].

Semiconductor laser is the fundamental device of modern optoelectronics and photonics.

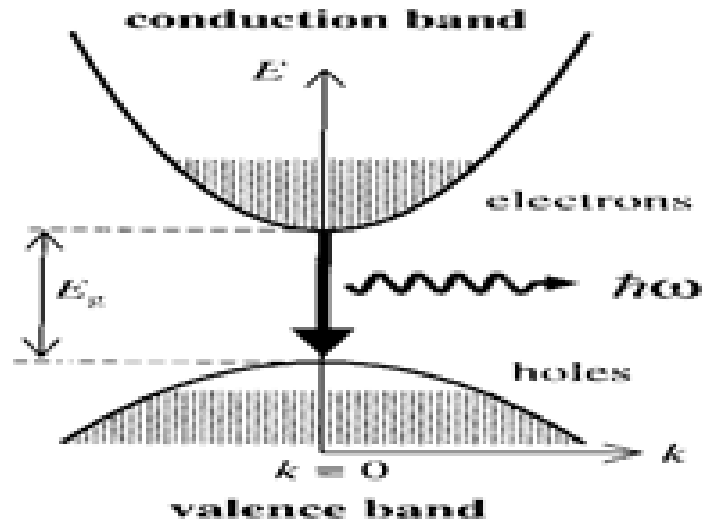


Figure 2.1: Direct band transition

Due to unique three dimensional quantum confinement, QD lasers have demonstrated both theoretically and experimentally many superior properties, such as ultra-low and temperature-stable threshold current density, high optical gain, high-speed operation, broad modulation bandwidth, and narrow spectrum line width primarily due to the delta-function like density of states [12].

The PL intensity of unstrained and intrinsic GaAs quantum dots were analyzed and theoretical reviewed in details.

In an indirect band materials, conservation of momentum requires that a phonon must either be emitted or absorbed when the photon is emitted. The interband luminescence in an indirect gap material is a second-order process. The R much more longer than for direct transition, therefore this makes the luminescence efficiency small. So the indirect gap materials such as silicon and germanium are generally band light emitters.

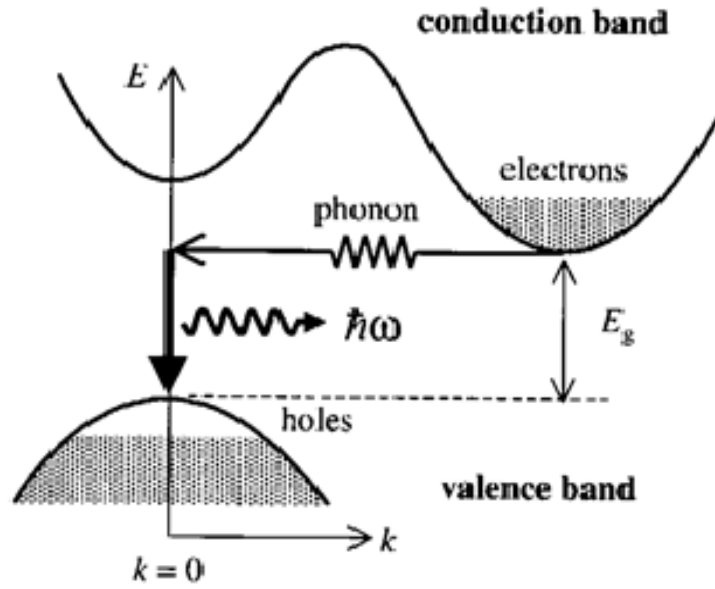


Figure 2.2: Indirect band transition

2.1.1 Fabrication of Semiconductor AlGaAs/GaAs Nanostructure

Synthesis of nanomaterials can be categorized as "Top-down" or "Bottom up" for such "Top-down" consists of removing material from bulk to form nanostructures whereas "Bottom up" approach involves atom by atom assembly on substrate [13]. Recently, unstrained $GaAs_x/Al_xGa_{1-x}As$ QDs were fabricated through an ingenious multistep approach based on a combination of hierarchical self-assembly and in situ etching.

For that purpose, the low density, high quality GaAs QDs were fabricated by droplet epitaxy in an AlGaAs matrix. The PL decay time of GaAs [14].

Due to the nonexistence of strain and reduced uncertainties in the size and shape, such QDs represent an ideal test case for electronic structure models. Let us shortly discuss the growth procedure of such unstrained.

First, a template of SK-grown InAs/GaAs (001) islands was created [15]. Then, the islands were "converted" into nanoholes on a GaAs surface by GaAs overgrowth followed

by in situ etching. Self-assembled nanoholes are then transferred to an AlGaAs surface, filled with GaAs, and finally overgrown with AlGaAs.

2.1.2 Application of AlGaAs/GaAs semiconductor nanostructure

Particular properties studied are its direct bandgap for photonic applications and its intervalley carrier transport and higher mobility for generating microwaves [16].

GaAs is a ubiquitous semiconductor in both scientific studies and in the semiconductors industry for several research.

GaAs has exceptionally large Bohr excitation diameter 22.4nm relative to other semiconductor allowing for the ease of experimental access to this fundamentally important threshold, similarly its high electron mobility $\frac{8500cm^2}{Vs}$ at room temperature is of the interest for electronic studies.

GaAs forms nearly strain free alloy with AlAs Further the GaAs alloy enables bandgap tunability across the range 1.42-2.2ev The combination of all these properties has enabled a variety of electronic and optoelectronic device, such as high electron mobility transistor (HEMT), Single photon source (SPS). Excitonic transistor (ET), and photo detector (PD), GaAs is well studied material system excessive photoluminescence at direct bandgap has inhibited analysis of resonance phenomena there [17]. There are a number of powerful experimental techniques that can be used to characterize structural and surface properties of nanomaterials either directly or indirectly, e.g. XRD (X-ray diffraction), STM (scanning tunneling microscopy), AFM (atomic force microscopy), SEM (scanning electron microscopy) [18].

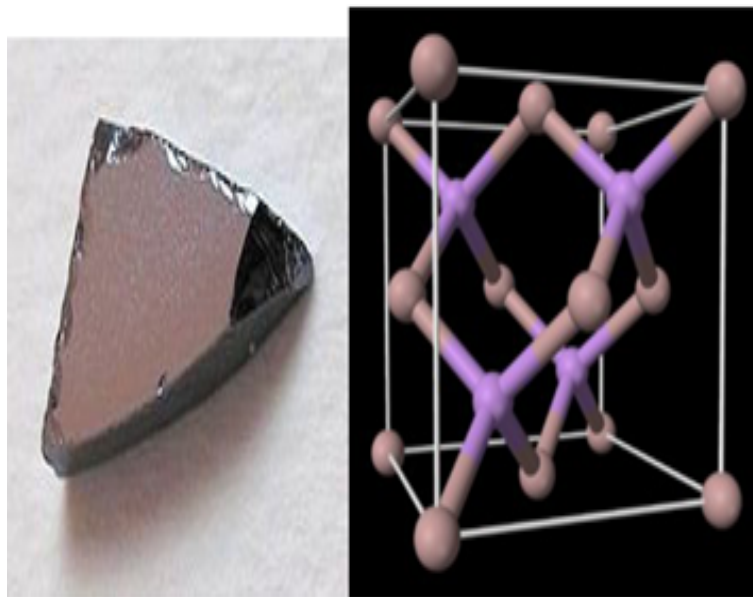


Figure 2.3: Band structure of Gallium arsenide (GaAs)

2.2 Quantum confinement and optical properties

2.2.1 Quantum Dots

Quantum dots (QD) are semiconductor nanostructures with vast applications across many industries. Their small size (2-10 nanometers or 10-50 atoms in diameter) gives quantum dots unique tunability. Like that of traditional semiconductors, the importance of QDs is originated from the fact that their electrical conductivity can be altered by an external stimulus such as voltage or photon flux [19].

One of the main differences between quantum dots and traditional semiconductors is that the peak emission frequencies of quantum dots are very sensitive to both the dot's size and composition.

A dot is a three dimensional object comprising several hundreds or thousands of atoms with finite shape. In quantum dots, the electrons are confined to a point in space. They have no freedom in any dimension and electrons are said to be localized at a point implying that a change in all directions changes the properties. They were discovered and

prepared at the beginning of the 1980s by Alexei Ekimov in a glass matrix and by Louis E. Brus in colloidal solutions [10].

Self-assembled (In,Ga)As/GaAs quantum dots (QDs) demonstrate many favorable physical properties that makes them suitable for numerous device applications the quantum dot is the ultimate nanostructure. All three degrees of freedom are quantum confined; therefore there is no plane-wave component of electron wave functions.

$$-\frac{\hbar\nabla^2}{2m}\psi(r) + V(r)\psi(r) = E(r)\psi(r) \quad (2.2.1)$$

The differential eq.(2.2.1) for a particle in 3D infinite trap of volume L^3 with impermeable walls with $V(r) = 0$ is given as:

$$\psi(x, y, z) = \left(\frac{2}{L}\right)^{\frac{3}{2}} \sin\left(\frac{n_x}{L}\pi x\right) \times \sin\left(\frac{n_y}{L}\pi y\right) \times \sin\left(\frac{n_z}{L}\pi z\right) \quad (2.2.2)$$

and the corresponding energy eigenvalue will be

$$E_n = \frac{\hbar^2\pi^2}{2m}(n_x^2 + n_y^2 + n_z^2) \quad (2.2.3)$$

Eqs.(2.2.2) and (2.2.3) are applicable to electron and hole states in semiconductor "quantum dots". A "hole"(missing electron) in a full energy band behaves very much like an electron except that it has a positive charge, and tends to float to the top of the band, i.e the energy of the hole increases oppositely to the energy of an electron. To create an electron hole pair in semiconductors requires energy at least equal to the energy gap of the semiconductor.

2.2.2 Quantum wires

Nanowires also called quantum wires are 1D molecular structure with electrical and or Optical properties. In order to have enhanced physical properties, the wires must be of small diameter, must have high aspect ratio i.e. the ratio of length to thickness, and must be uniformly oriented.

Nanowires are relatively easy to produce and can have, and they are often thin and short

”threads” but can also have other manifestations. The propagation of electromagnetic energy has been demonstrated along a noble metal stripes with band of a few microns, propagation has also been demonstrated along nanowires with sub wavelength cross sections and propagation length of a few micron. Metal nanowires can also be used to ”transmit” photons. The optical properties of metal nanowires can be optimized for particular wavelength of interest, and non-regular cross-sections and coupling between closely spaced nanowires allows a tunneling of optical response. The solution of eq.(2.2.1) in the case of quantum wire of a square cross-section is and the Corresponding band structure is given as,

$$\psi(x, y, z) = \left(\frac{4}{L}\right)^{\frac{1}{2}} \sin\left(\frac{n_x}{L}\pi x\right) \times \sin\left(\frac{n_y}{L}\pi y\right) \quad (2.2.4)$$

Corresponding energy is

$$E_n = \frac{\hbar^2 \pi^2}{2m} (n_y^2 + n_z^2) + \frac{\hbar^2 k_x^2}{2m} \quad (2.2.5)$$

Multiple subbands are formed, similar to the quantum well structure. A new subband Forms at each eigenvalue $E(n_x, n_y)$, and each subband has a dispersion $E(n_k) = \frac{\hbar^2 k_z^2}{2m_z}$.

2.2.3 Quantum Wells.

Quantum wells are formed upon sandwiching a thin layer of semiconductor between wider bandgap barrier layers. The finite extent of the quantum well layer makes the conduction band profile mimic a one-dimensional quantum well in the direction of growth (x-direction), leaving motion in the y -z plane free. Thus, the square-well potential (with reference to the conduction band edge E_{co}) is written as

$$V(x, y, z) = 0, x < 0, V(x, y, z) = 0, x > L, V(x, y, z) = -\Delta E_c, 0 \leq x \leq L \quad (2.2.6)$$

A physical situation that often arises in semiconductor devices is a carrier confined in one dimension, says Z to a thickness d and free in two dimensions say x and y this is called 2D bands or quantum wells. In this case the solution of eq.(2.2.1) will have the form

$$\psi_n(x, y, z) = \sqrt{\frac{2}{L}} \left(\sin \frac{n_z \pi z}{L} \right) \quad (2.2.7)$$

and the energy of the carrier in the n^{th} and

$$E_n = \frac{\hbar^2}{2mL^2}n_z^2 + \frac{\hbar^2 k_x^2}{2m} + \frac{\hbar^2 k_y^2}{2m} \quad (2.2.8)$$

2.3 Density of states

2.3.1 Density of states Bulk

First, let us derive the bulk density of states. There exist a number of approaches for doing this. In fact, we have used here one simplest method which easy and understandable. The total volume of sphere considered k space given by

$$V_k = \frac{4}{3}\pi k^3 \quad (2.3.1)$$

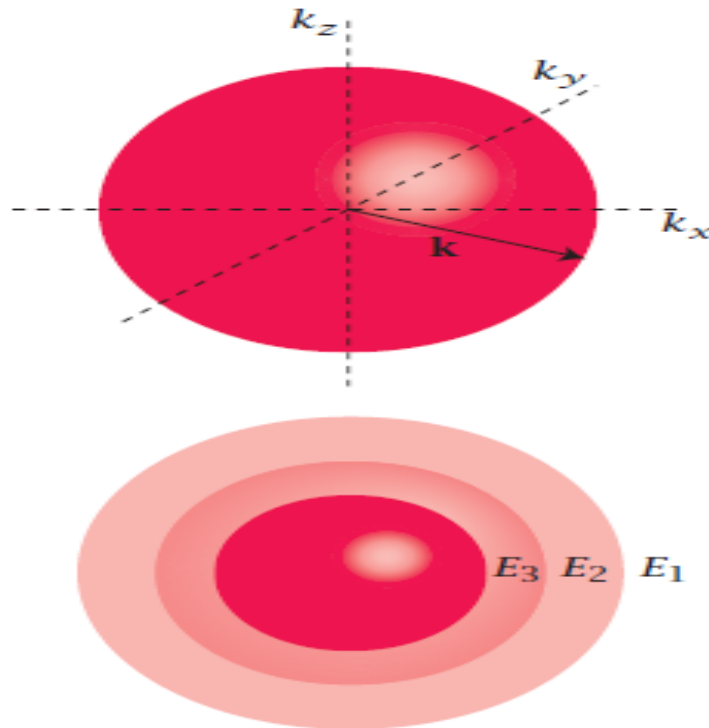


Figure 2.4: Constant-energy spherical surfaces in k-space

Where k_{radius} of and $k^2 = k_x^2 + k_y^2 + k_z^2$, $k_x = \frac{2\pi n_x}{L_x}$, $k_y = \frac{2\pi n_y}{L_y}$, and $k_z = \frac{2\pi n_z}{L_z}$, (where $n_x, n_y, n_z = 0 \pm 1, \pm 2, \pm 3 \dots$) Notice also that in a cubic solid, $L_x = L_y = L_z = Na$, where

N is the number of unit cells along a given direction and a represents an interatomic spacing. The above volume contains much energy, since $E = \frac{\hbar^2 k^2}{2m^*} = \frac{p^2}{2m^*}$ Figure 2.4 Constant energy spherical surfaces in k -space. Different radii (K) Furthermore, every point on the sphere's surface possesses the same energy. Spheres with smaller radii therefore have points on their surfaces with equivalent, but correspondingly smaller, energies. This is illustrated in We now define a state by the smallest nonzero volume it possesses in k -space. This occurs when $k_x = \frac{2\pi}{L_x}, k_y = \frac{2\pi}{L_y}$ and $k_z = \frac{2\pi}{L_z}$ so that

$$V_{state} = k_x k_y k_z = \frac{8\pi^3}{L_x L_y L_z} \quad (2.3.2)$$

Thus, within our imagined spherical volume of k -space, the total number of states present is

$$N_1 = \frac{V_k}{V_{state}} = \frac{4\pi k^3}{3k_x k_y k_z} = \frac{k^3 L_x L_y L_z}{6\pi^2} \quad (2.3.3)$$

Next, when dealing with electrons and holes, we must consider spin degeneracy, since two carriers, possessing opposite spin, can occupy the same state. As a consequence, we multiply the above expression by 2 to obtain

$$N = 2N_1 = \frac{k^3 L_x L_y L_z}{3\pi^2} \quad (2.3.4)$$

This represents the total number of available states for carriers, accounting for spin. We now define a density of states per unit volume, $\rho = \frac{N_2}{L_x L_y L_z}$, with units of number per unit volume. These results in

$$\rho = \frac{k^3}{3\pi^2} \quad (2.3.5)$$

Finally, considering an energy density $\rho_{energy} = d\rho/dE$, with units number per unit energy per unit volume, we obtain

$$\rho_{Energy} = \frac{d}{3\pi^2 dE} \left(\frac{2m^* E}{\hbar^2} \right)^{\frac{3}{2}} \quad (2.3.6)$$

which simplifies to

$$\rho_{energy} = \frac{(2m^*)^{\frac{3}{2}}}{2\pi^2 \hbar^3} \sqrt{E} \quad (2.3.7)$$

This is our desired density-of-states expression for a bulk three dimensional solid. Note that the function possesses characteristic square root energy dependence.

2.3.2 Density of States of Quantum Well, Quantum wires and Quantum dots

The density of states of a quantum well

As with the bulk density of states evaluation, there are various approaches for doing this. We begin with one which is simpler to be understandable. The one direction of

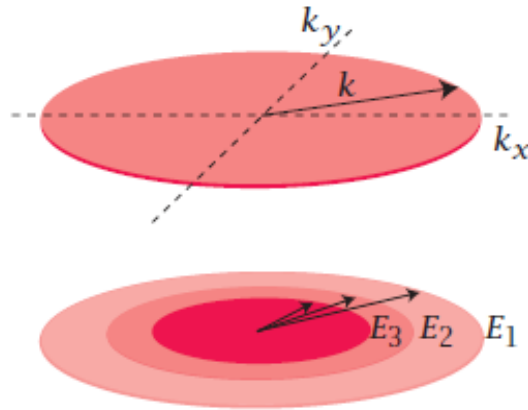


Figure 2.5: Constant-energy perimeters in k-space. the (x, y) plane.

confinement that occurs along the z direction is excluded. The associated circular area in k-space is then

$$A_k = \pi k^2 \quad (2.3.8)$$

and encompasses many states having different energies. A given state within this circle occupies an area of

$$A_{state} = k_x k_y \quad (2.3.9)$$

with $k_x = \frac{2\pi}{L_x}$ and $k_y = \frac{2\pi}{L_y}$. Recall that $L_x = L_y = Na$ where N is the number of unit cells along a given direction and a represents an interatomic spacing. Thus,

$$A_{state} = \frac{(2\pi)^2}{L_x L_y} \quad (2.3.10)$$

The total number of states encompassed by this circular area is therefore $N_1 = \frac{A_k}{A_{state}}$, resulting in

$$N_1 = \frac{k^2}{4\pi} L_x L_y \quad (2.3.11)$$

If we account for spin degeneracy, this value is further multiplied by 2, $N_2 = 2N_1$ Then

$$N_2 = \frac{k^2}{2\pi} L_x L_y \quad (2.3.12)$$

giving the total number of available states for carriers, including spin. At this point, we can define an area density

$$\rho = \frac{N_2}{L_x L_y} = \frac{k^2}{2\pi} = \frac{2m^* E}{\pi \hbar^2} \quad (2.3.13)$$

with units of number per unit area, since $k = \sqrt{\frac{2m^* E}{\hbar^2}}$ Our desired energy density is then $\rho_{energy} = \frac{d\rho}{dE}$ and yields.

$$\rho_{energy} = \frac{m^*}{\pi \hbar^2} \quad (2.3.14)$$

with units of number per unit energy per unit area. Notice that it is a constant. Notice also that this density of states in (x, y) accompanies states associated with each value of k_z (or n_z). As a consequence, each k_z (or n_z) value is accompanied by a "subband" and one generally expresses this through.

$$\rho_{energy}(E) = \frac{m^*}{\pi \hbar^2} \delta(E - E_z) \quad (2.3.15)$$

where n_z is the index associated with the confinement energy along the z direction and $\theta(E - E_{n_z})$ is the Heaviside unit step function, defined by $\theta(E - E_{n_z}) = 0, if E < E_{n_z}$ and $\theta(E - E_{n_z}) = 1, if E > E_{n_z}$

Density of States Quantum wires

. The derivation of the nanowire density of states proceeds in an identical manner. The only change is the different dimensionality. Whereas we discussed volumes and areas for bulk systems and quantum wells, we refer to lengths here. As before, there are also alternative derivations. One of these is presented in an optional section and can be skipped

if desired. For a nanowire, consider a symmetric line about the origin in k-space having length $2k:L_k = 2k$. The associated width occupied by a given state is $L_{state} = k$ where k represents any one of three directions in k-space: k_x, k_y or k_z . For convenience, choose the z direction. This will represent the single degree of freedom for carriers in the wire. We then have possible k_z values of

$$k_z = \frac{2\pi n_z}{L_z} \quad (2.3.16)$$

with $n_z = 0, \pm 1, \pm 2, \pm 3, \dots$ where $L_z = Na$ where N represents the number of unit cells along the z direction, and a is an interatomic spacing. The smallest nonzero length occurs when $n_z = 1$. As a consequence, the number of states found within L_k is

$$N_1 = \frac{L_k}{L_{state}} = \frac{kL_z}{\pi} \quad (2.3.17)$$

if spin degeneracy is considered $N_2 = 2N_1 \frac{2kL_z}{\pi}$ and describes the total number of available states for carriers. We now define a density

$$\rho = \frac{N_2}{L_z} = \frac{2\sqrt{2m^*E}}{\rho} \quad (2.3.18)$$

that describes the number of states per unit length, including spin. This leads to an expression for the DOS defined as $\rho_{energy} = \frac{d\rho}{dE}$ thus $\rho_{energy}(E) \frac{2dk}{\pi dE}$ giving

$$\rho_{energy} = \frac{1}{\pi} \sqrt{\frac{2m^*}{\hbar^2}} \frac{1}{\sqrt{E}} \quad (2.3.19)$$

Equation (2.3.19) is our desired expression, with units of number per unit energy per unit length. More generally, since this distribution is associated with confined energies along the other two directions, y and z, we write

$$\rho_{energy}(E) = \frac{1}{\pi} \sqrt{\frac{2m^*}{\hbar^2}} \sum_{n_x, n_y} \frac{1}{\sqrt{E - E_{n_x, n_y}}} \quad (2.3.20)$$

Where E_{n_x, n_y} are the confinement energies associated with the x and y directions and $\theta(E - E_{n_x, n_y})$ is the Heaviside unit step function. Notice the characteristic inverse square root dependence of the nanowire one dimensional density of states.

Quantum Dot Density of States

Quantum dot, the density of states is just a series of delta functions, given that all three dimensions exhibit carrier confinement:

$$\rho_{energy}(E) = 2\sigma(E - E_{n_x n_y n_z}) \quad (2.3.21)$$

In Equation(2.1.21) E_{n_x, n_y, n_z} are the confined energies of the carrier, characterized by the indices n_x, n_y, n_z . The factor of 2 accounts for spin degeneracy. To generalize the expression, we write

$$\rho_{energy}(E) = 2 \sum_{n_x, n_y, n_z} \sigma(E - E_{n_x n_y n_z}) \quad (2.3.22)$$

This accounts for all the confined states in the system

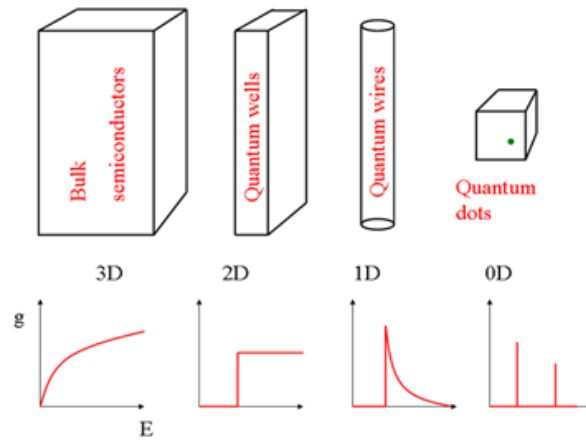


Figure 2.6: Reduction of the dimensionality of semiconductor system from 3D to 0D

2.3.3 Population of the conduction band

Whether for the electron or the hole, the above density of-states expressions just tell us the density of available states. They say nothing about whether or not such states are occupied. For this, we need the probability $P(E)$ that an electron or hole resides in a given state with an energy E . This will therefore be the focus of the current section and is also our first application of the density-of-states function to find where most carriers

reside in a given band. Through this, we will determine both the carrier concentration and the position of the so-called fermi level in each system. Let us first consider a bulk solid. We begin by evaluating the occupation Let us first consider a bulk solid. We begin by evaluating the occupation of states in the conduction band, followed by the same calculation for holes in the valence band.

Conduction Band and valence band in bulk

For the conduction band, we have the following expression for the number of occupied states at a given energy per unit volume (alternatively, the concentration of electrons at a given energy).

Conduction Band in bulk

$$dn_e(E) = P_e \rho_{energy}(E) dE \quad (2.3.23)$$

In this expression, P_e is the probability that an electron possesses a given energy E and is called the Fermi-Dirac distribution.

$$P_e(E) = \frac{1}{1 + \exp\left(\frac{E-E_F}{k_B T}\right)} \quad (2.3.24)$$

There are several things to note. First, E_F refers to the Fermi level, which should be distinguished from the Fermi energy. The total concentration of electrons in the conduction band n_c is then the integral of $n_e(E)$ over all available energies:

$$n_c = \int_{E_c}^{\infty} P_e(E) \rho_{energy}(E) dE \quad (2.3.25)$$

Notice that the lower limit of the integral is E_c , which represents the starting energy of the conduction band. We have previously found for bulk materials equation(2.3.25) that $\rho_{energy} = \frac{1}{2\pi^2} \left(\frac{2m^*}{\hbar^2}\right) \sqrt{E}$ we can substitute for the m^* effective mass by the m_e^*

$$\rho_{energy}(E) = \frac{1}{2\pi^2} \frac{2m_e^*}{\hbar^2} \sqrt{E} \quad (2.3.26)$$

Inserting this into our integral then yields

$$n_c = \int_{E_c}^{\infty} \frac{1}{1 + \exp\left(\frac{E-E_F}{K_B T}\right)} \frac{(\hbar^2)^{\frac{3}{2}} \sqrt{E - E_c} dE}{2m_e} \frac{1}{2\pi^2} \quad (2.3.27)$$

The resulting integral has been solved and can be looked up. It is called the incomplete Fermi-Dirac integral and is defined as follows:

Valance Band in bulk

$$n_v = \int_{\infty}^{E_v} P_h(E) \rho_{energy}(E) dE \quad (2.3.28)$$

$$n_v = \int_{\infty}^{E_v} \left(1 - \frac{1}{1 + \exp\left(\frac{E_F - E}{K_B T}\right)}\right) \sqrt{E_v - E} dE \quad (2.3.29)$$

Conduction band in Quantum well

$$n_c = \frac{m_e k_B T}{\pi \hbar^2 \exp\left(\frac{E_{nc} - E}{K_B T}\right)} \quad (2.3.30)$$

Valance band in Quantum well

$$n_v = \frac{m_h k_B T}{\pi \hbar^2 \exp\left(\frac{E_F - E_{nh}}{K_B T}\right)} \quad (2.3.31)$$

conduction band in Quantum wire

$$n_c = \frac{1}{\pi} \sqrt{\frac{m_e}{\hbar^2}} \exp\left(-\frac{E_{n_x, e, n_y, e} - E_F}{K_B T}\right) \int_{E_{n_x, e, n_y, e}}^{\infty} \exp\left(\frac{-E - E_{n_x, e, n_y, e}}{K_B T}\right) \frac{1}{\sqrt{E - E_{n_x, e, n_y, e}}} dE \quad (2.3.32)$$

2.3.4 Fermi Level

We can now determine the location of the fermi level E_F from n_v and n_c , assuming that the material is intrinsic (i.e., not deliberately doped with impurities to have extra electrons or holes in it). We will also assume that the material is not being excited optically, so that the system remains in thermal equilibrium. Under these conditions, the following equivalence holds, since associated with every electron is a hole: $n_c = n_v$

$$N_v \exp\left(\frac{-(E_c - E_F)}{K_B T}\right) = N_h \frac{-E_F - E_v}{k_B T} \quad (2.3.33)$$

Thus the fermi level in intrinsic semiconductor nanostructures

$$E_F = \frac{E_c + E_v}{2} + \frac{3}{4}k_B T \ln\left(\frac{m_h}{m_e}\right) \quad (2.3.34)$$

solving for fermi energy which says that at $T = 0$ K, the Fermi level of an intrinsic semiconductor at equilibrium occurs halfway between the conduction band and the valence band. However, a weak temperature dependence exists, moving the fermi level closer to the conduction band when $m_h > m_e$. Alternatively, if $m_e > m_h$ the fermi level moves closer to the valence band. To a good approximation, the fermi level lies midway between the two bands, $\frac{3}{4}k_B T \ln \frac{m_h}{m_e}$ is scaling factor for GaAs it is equal to $35mev$ in which $E_g = 1.42ev$

2.4 Dynamics of charge carriers in semiconductor nanostructures

Shining light on semiconductors causes the following elementary excitations: Interband transitions, excitonic transitions or below-bandgap transitions. These processes are for direct bandgap material, i.e. the conduction band minimum occurs at the same position in k-space as the valence band maximum. If the photon energy is larger than the bandgap, interband transitions dominate, exciting electrons from the valence into the conduction band. The free electron and hole concentrations in bulk semiconductors can be modified by the processes of generation and recombination, and also by the transport of electrons and holes through drift and diffusion. Generation: absorption of a photon generates a free electron and a free hole (electron-hole pair).

Recombination is often considered to be the time reversed process of absorption, however, the processes are not identical.

Absorption can take place into any excited state above the Fermi energy, whereas, recombination can only occur from a small range of relaxed states above the Fermi energy. As with absorption, recombination processes can occur as inter-band, intra-band, direct and indirect transitions [20]. It can be radiative, in which case a photon is emitted

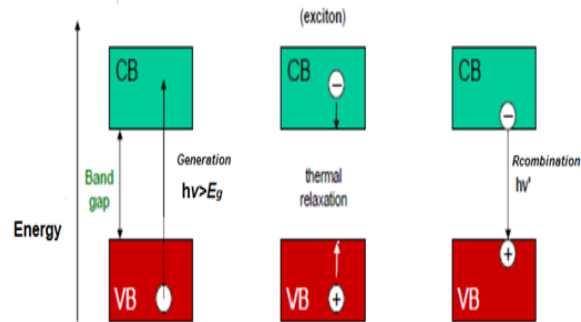


Figure 2.7: (Generation, Relaxation and Recombination.)

as the electron returns to the valence band, or non-radiative, in which case the energy associated with the e-h pair is converted to heat, or transferred to another charge carrier (Auger recombination) non radiative corresponds to no photon. Charge carriers move be-

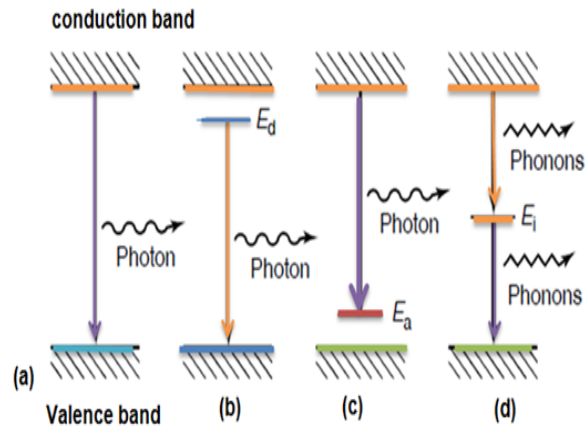


Figure 2.8: (a-c) Radiative recombination paths: (a) band-to band; (b) donor to valence band; (c) conduction band to acceptor. (d) Nonradiative recombination via an intermediate state.

tween valence and conduction bands under thermal influence (thermal excitation within the Boltzmann tail of the Fermi Dirac distribution). In the dark and at equilibrium, the concentration of electrons and holes are unaffected by these processes Generation, under

influence of light absorption for example, promotes electrons from the valence band to the conduction band, resulting in a new free electron in the CB, and a new hole in the VB. Relaxation (thermalisation) processes occur after optical excitation of an electron into a higher energy state. This is the process by which the electron temperature equilibrates with the lattice temperature. The electron in the excited state and associated hole in the ground state relax their energy by scattering into different momentum states through a series of processes. These processes include; interactions with the lattice (phonons), grain boundaries, surface defects or through interactions with other electrons in non radiative processes. The carriers have well-defined phase relationships with each other and with the external field. This coherence is lost due to various efficient scattering mechanisms(e.g. momentum, carrier-carrier and hole-optical-phonon scattering) [21]. Phases of the individual carriers are changed and only within a time range of only a few tens to hundreds femtoseconds, which is referred to as dephasing.

2.4.1 Radiative recombination

When an electron relaxes from the conduction into the valence band to recombine with a hole, energy is released in form of a photon. This can happen either spontaneously with recombination rate.

2.4.2 Nonradiative recombination

Nonradiative recombination Creating photons is not the only way of releasing energy when electrons and holes recombine. Alternative processes are called nonradiative, since no photons are emitted. They can be categorized into Auger recombination and recombination at defect or surface states, In an Auger processes a carrier transfers its momentum and energy to a third carrier. With the usual notation of n and p for electron and hole densities, the recombination rate is therefore proportional to depending on the carriers involved. It is hence obvious that Auger processes will be primarily important for high carrier densities. They are furthermore bandgap dependent and increase exponentially as

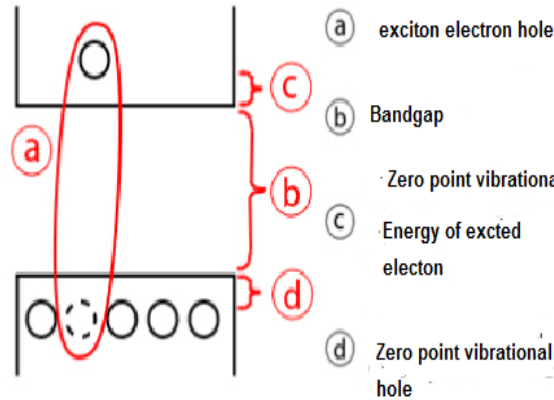


Figure 2.9: Exciton of electron-hole.

the bandgap is decreased.

$$R_{Auger} \propto n^2 P \text{ or } R_{Auger} \propto np^2 \quad (2.4.1)$$

2.4.3 Excitons

When electron-hole pair is created by absorption of a photon inside a semiconductor, the pair experiences an attractive Coulomb force. The latter is responsible for the creation of a bound state called an exciton. The exciton can be loosely described by a Hydrogen-like system where electrons and holes orbit around their center-of-mass. One distinguishes in the literature two types of excitons, depending essentially on the ratio of the exciton radius to the lattice spacing. When the attraction is so strong that the radius of the exciton is of the same order as the lattice spacing, one refers to a Frenkel exciton. Because of the small effective mass and the dielectric constant of the semiconductors, the exciton in a semiconductor is rather of the Wannier type, where the exciton radius is of many lattice periods. The simplest excitation in semiconductors occurs when electrons from the valence band jump across the band gap into the conduction band. In this case an empty positively charged state is created with the valence band named hole having charge positive. The electron and holes are bound by the coulomb interaction. This bound

electron-hole state is known as exciton [21]. We can derive from hydrogen model binding energy The centrifugal force, $F_C = \frac{mv^2}{r}$ and Electrostatic force $F_e = \frac{e^2}{4\pi\epsilon_o}$ By stability condition $F_c = F_e$

$$E_p + E_k = -\frac{e^2}{4\pi\epsilon_o} - \frac{e^2}{4\pi\epsilon_o} = -\frac{e^2}{8\pi\epsilon_o} < 0 \quad (2.4.2)$$

Free exciton binding energy Hamiltonian

$$H = \frac{p_e^2}{2m_e^*} + \frac{p_h^2}{2m_h^*} - \frac{e^2}{4\pi\epsilon_o(r_e - r_h)} \quad (2.4.3)$$

This electrostatic interaction can lead to composite particles, so called excitons that are often compared to hydrogen atoms because of their similar energy structures.

$$H = \frac{\hbar^2\nabla^2}{2m_e^*} - \frac{\hbar^2\nabla^2}{2m_h^*} - \frac{e^2}{4\pi\epsilon(r_e - r_h)} \quad (2.4.4)$$

Which consists of the kinetic terms for electron and hole respectively and the Coulomb interaction between the two. Here m_e^* and m_h^* are the effective masses for electron and hole respectively, e is the elementary charge, ϵ_o is the permittivity of the material and r_e, r_h are the position vectors for electron and hole. The analogy to the hydrogen atom becomes and we can adapt its solution by taking into account the effective masses and the dielectric constant of the crystal. The Coulomb interaction results in the following excitonic energy eigenvalues:

$$E_n = \frac{R_y^*}{n^2} \quad (2.4.5)$$

Being the Rydberg energy (ground state energy) of the exciton. In equation (2.4.5) we make use of the expression

$$\alpha_B = \frac{4\pi\epsilon\hbar^2}{\mu e^2} \quad (2.4.6)$$

for the radius of the exciton $\frac{1}{\mu} = \frac{1}{m_e^*} + \frac{1}{m_h^*}$ the reduced mass exciton) which follows the well-known definition of the Bohr radius in the case of the hydrogen atom. If the exciton is created through the absorption of a photon we can derive for its total energy:

$$E_{ex} = E_g - \frac{R_y^*}{n^2} \quad (2.4.7)$$

which does not comprise a kinetic term as the photon possesses negligibly small momentum. Because of the effective masses in equation (2.4.4) being smaller than the electron mass, exciton radii are of the range of several nanometers.

The charge carriers therefore are delocalized over several thousand crystal lattice points. This kind of exciton is called a Wannier-Mott-exciton in contrast to Frenkel-excitons which are strongly localized electron-hole-pairs.

The Rydberg energy of excitons on the other hand is smaller than for the hydrogen atom and lies in the range of 1 -100meV. The exciton binding energy of GaAs is about 4.2 eV

2.5 Photoluminescence

The mechanism involves effectively pinning the minority excess carrier density, resulting in a dependence of the photoluminescence intensity on only the majority carrier density [1]. During the last four decades, Photoluminescence spectroscopy has been extensively used as characterized tools for fundamental research. However, because of the importance of high quality materials and material structure, especially in the case of semiconductors, such as quantum wells (QWs), quantum wires (QWRs) and quantum dots (QDs), fundamental research and material characterization are not separable.

Photoluminescence (PL) is the spontaneous emission of light from a material under optical excitation. The excitation energy and intensity are chosen to probe different regions and excitation concentrations in the sample. PL investigations can be used to characterize a variety of material parameters. PL spectroscopy provides electrical (as opposed to mechanical) characterization, and it is a selective and extremely sensitive probe of discrete electronic states.

Photoluminescence intensity

The intensity of the PL signal has received the most attention in the analysis of interfaces. This interest is due to the fact that, although several important mechanisms affect the PL response, it is generally found that large PL signals correlate with good interface

properties [1]. Features of the emission spectrum can be used to identify surface, interface,

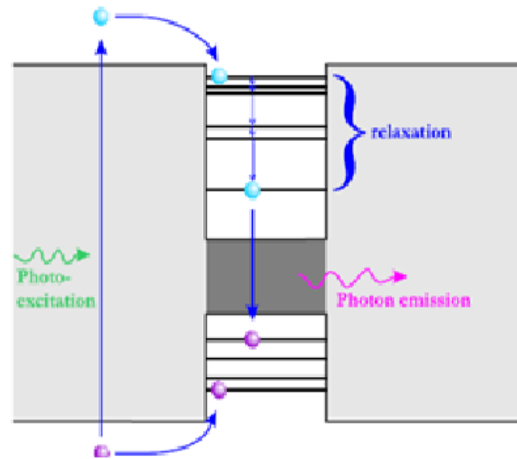


Figure 2.10: Processes involved in a photoluminescence experiment. The non-resonant photons are absorbed, creating hot electrons and holes

and impurity levels and to gauge alloy disorder and interface roughness. The intensity of the PL signal provides information on the quality of surfaces and interfaces. Under pulsed excitation, the transient PL intensity yields the lifetime of nonequilibrium interface and bulk states.

Variation of the PL intensity under an applied bias can be used to map the electric field at the surface of a sample. In addition, thermally activated processes cause changes in PL intensity with temperature. PL analysis is nondestructive. Indeed, the technique requires very little sample manipulation or environmental control [1]. Because the sample is excited optically, electrical contacts and junctions are unnecessary and high-resistivity materials pose no practical difficulty. In addition, time-resolved PL can be very fast, making it useful for characterizing the most rapid processes in a material. PL spectrum color depend on the size of QDs that inform us the other optical properties of semiconductor nanostructures

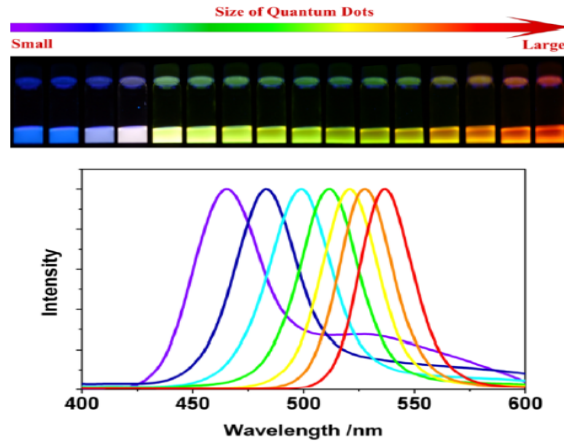


Figure 2.11: schematically diagram depict Size dependent of PL in (from left to right size decreasing blue shift spectrum)

2.6 Analytical Calculation of optical parameters on photoluminescence intensity

2.6.1 Temperature dependence of PL emission

The overall shift of the QD emission to lower energies is caused by bandgap narrowing. The PL spectrum red-shifts faster than the band gap of the material. At low temperature ($T < 100K$) the carriers are captured by all the QDs randomly. Once captured the carriers in the QDs cannot be thermally excited out [22].

So the emission reflects the natural distribution of the QD. Irrespective of the specific quenching mechanism, the temperature dependence of the integrated intensity $I(T)$ of PL bands in GaAs is most often described by the expression with the process rate parameter α and activation energy E_T . As a rule, expression. QDs are preferentially captured by larger QDs that have an increased confinement potential.

As the carriers populate these QDs more readily the energy of emission decreases, so a red-shift that is of greater magnitude than the bandgap red-shift is observed. At higher temperatures, up to $300K$ ($35mev$), the thermal distribution of carriers causes the higher excited state energy levels to become optically active and broadens the emission. Carriers

are easily excited to higher states inside the QD and thermally ionized from the QD. This results in a quenching of the emission and a widening of the linewidth [23].

$$I(T) = \frac{I_o}{1 + C \exp\left(\frac{-\Delta E}{k_B T}\right)} \quad (2.6.1)$$

Temperature dependence photoluminescence spectroscopy (PL) is powerful optical method used for characterizing materials. Temperature dependent PL measurements are particularly useful in characterizing material containing quantum dots and quantum wells assist in optimization of the specific characteristics of the InGaAs/GaAs quantum dots molecules describe above typically one of two types cryostat are used.

A cryostat requiring liquid and /or liquid helium or closed cycle cryostat in which a cryogenic liquid is included as a part of cooling system. The cooled sample is excited by laser and PL emission is cooled to spectrometry via an optical interference [24]. The basic principle of the method is similar to that of the DLTS. If the measurement temperature of the PL is 0K, electrons and holes that are generated by external light pumping cannot escape from the QDs or the QWs; thus, generated electrons and holes are recombined in the quantum structures, and the integrated PL intensity I_0 is larger than that measured at any other temperature. When the measurement temperature becomes higher, the carriers in the quantum structures are affected by thermal activation energy, and they start to escape from the quantum structures due to the activation energy E_a ; thus the integrated PL intensity becomes lower. The temperature dependent integrated PL intensity(I) [1], follows the equation(2.6.1)

2.6.2 Optical Absorption and emission

Macroscopic absorption coefficient α : the sum of the absorption cross section per unit volume of material for the various optical processes. It describes how the light intensity is attenuated on passing through the material schematically diagram of material absorption

$\frac{dI(z)}{dz} = -\alpha I(z)$ For a material of non-uniform α the intensity at α depth z , is given by

$$I(Z) = I_o \exp \int_0^z \alpha(E, z) dz \quad (2.6.2)$$

where, $I(0)$ is the intensity just inside the interface. For uniform α , that is the simple Beer-Lambert law.

$$I(z) = I_o \exp(-\alpha z) \quad (2.6.3)$$

Where $I(z)$ is the intensity transmitted through the sample of thickness z , and $I(0)$ is the incident light intensity.

The absorption coefficient α strongly depends on wavelength. Semiconductors can have absorption up to 10^5 cm^{-1} for photons with energies above the bandgap, and very low absorption for photons having energy below the bandgap. A semiconductor is characterized by a valence band that is filled by electrons and a conduction band that is separated in energy by an amount E_g , the bandgap, from the upper edge of the valence band.

Semiconductors are transparent to photons whose energies lie below their bandgap and are strongly absorbing for photons whose energies exceed the bandgap energy.

2.6.3 The quantum confinement model (QCM)

The development of this model is based on the effective mass approximation theory. In this model, the luminescence process is attributed to an energy shift of carriers (electrons and holes) and is proportional to the photon energy emitted would be slightly larger than the bandgap energy. The size dependence of the photoluminescence (PL) intensity of decay time of unstrained GaAs quantum dot (QD) ensembles grown on an $Al_{0.3}Ga_{0.7}As/GaAs$ (100) surface by using droplet epitaxy. The density of GaAs QDs is $3 \times 10^9 / \text{cm}^2$, which indicates that each QD is isolated from neighboring QDs. The low-temperature PL spectrum of the GaAs QD ensembles shows a Gaussian profile with a linewidth broadening of 30 nm [24]. We analyze here the spectrum of the spontaneous emission. Near the band edges, the

energy of the emitted photon is governed by the relationship [25]

$$h\nu = \hbar\omega = E_c + \frac{\hbar^2 k^2}{2m_e^*} - (E_v - \frac{\hbar^2 k^2}{2m_v^*}) \quad (2.6.4)$$

The above is called the joint dispersion relation and m_r^* ; is the reduced effective mass

$$\frac{1}{m_r^*} = \frac{1}{m_e^*} + \frac{1}{m_h^*} \quad (2.6.5)$$

With similar treatment, a joint density of states can be obtained as

$$\rho_{energy}(E) = \frac{(2m_r^*)^{\frac{3}{2}}}{2\pi^2\hbar^3} \sqrt{E - E_g} \quad (2.6.6)$$

The distribution of carriers is governed by the Boltzmann distribution

$$F(E) = \exp\left(\frac{-E}{k_B T}\right) \quad (2.6.7)$$

The spontaneous emission rate is proportional to the product of Eqs. (2.6.7) and (2.6.8) it generally has the form [26]

$$I(h\nu) \propto \sqrt{E - E_g} \exp\left(\frac{-E}{k_B T}\right) \quad (2.6.8)$$

$$I(E) = \gamma \sqrt{E - E_g} \exp\left(\frac{-E}{k_B T}\right), \text{ where, } \gamma = \frac{(2m_r^*)^{\frac{3}{2}}}{2\pi^2\hbar^3} \quad (2.6.9)$$

According to the QC model, the emission wavelength and intensity depends on nanocrystal diameter, size distribution and concentration. This model can explain the general tendency of most experimental results such as the blue shift of the luminescence spectrum with decrease of the GaAs-nc size. A natural choice to find QDs size is to associate the effective size with the diameter of the sphere of bulk GaAs and contains the same number of GaAs clusters as the QD [27]. Some experimental evidence for quantum size effects in confined excitons was obtained by Ekimov and Onushchenko in 1981. Their model was based on the effective mass approximation (EMA). In the weak confinement regime the

dominant energy term is the Coulomb term, and quantization of the motion of the exciton occurs. The shift in energy of the lowest energy state is [28]

$$\Delta E = \frac{\hbar^2 \pi^2}{2MR^2} \quad (2.6.10)$$

Weak confinement

where M is the mass of the exciton and is given by $M = m_e^* + m_h^*$. The electrons and holes can now be thought of as independent particles; excitons are not formed. Separate quantization of motion of the electron and hole is now an important factor. The optical spectra should consist of a series of lines due to transitions between subbands. The shift in energy is now

$$\Delta E = \frac{\hbar^2 \pi^2}{2\mu R^2} \quad (2.6.11)$$

Strong confinement

Where the excitonic mass is now replaced by the reduced mass μ . In the weak confinement regime the dominant energy term is the Coulomb term, and quantization of the motion of the exciton occurs. The shift in energy of the lowest energy state is

$$\Delta E = \frac{\hbar^2 \pi^2}{2m_e^* R^2} \quad (2.6.12)$$

very small nanoclusters. The extension of the Efros and Efros model by Brus and by Kayanuma to include Coulomb and correlation energy terms enables derivation of an expression that models energies and provides a reasonable guide to cluster size as a function of E_g . Assuming that a Gaussian size distribution about the mean diameter d_0 for the nanocrystallites [28]

$$I(d) = \frac{1}{\sqrt{2\pi}\sigma} \text{Nexp} \left(\frac{(d - d_0)^2}{2\sigma^2} \right) \quad (2.6.13)$$

The number of electrons N in a column diameter d participating in the PL process is proportional to d^2 . The heights of the columns depend only on the growth time and are approximately the same.

2.6.4 Time Resolved

Which of the three explanations is the true scenario can be decided on the basis of resonant and non-resonant time-resolved (T_R) PL studies (for clarity: Resonant excitation means, that the excitation energy is equal to the detection energy and for non-resonant excitation the excitation energy is larger than the bandgap of the GaAs matrix material) For a QW structure, resonant PL measurements within the continuum of the emission peak should reveal short lifetimes as carriers can relax instantly into QW states of lower energy because of the continuous density of states. Under resonant excitation of an ensemble of QDs with a σ -function-like density of states, the carriers are lifted directly into the ground state and long lifetimes will be observed, similar to non-resonant excitation. Time-resolved photoluminescence experiments samples are excited with ultra short light pulses and the change of the emitted light as a function of time is monitored [29]. To gain information about the carrier dynamics it is therefore necessary to find the relationship between the photoluminescence decay and the carrier lifetimes The photoluminescence intensity, i.e. the light signal emitted by the material due to radiative recombination, is proportional to the product of electron and hole concentrations [2]

$$\frac{1}{\tau_{capt}} = \frac{1}{\tau_p} + \frac{1}{\tau_n} \quad (2.6.14)$$

and

$$\frac{1}{\tau_{PL}} = \frac{1}{\tau_{rad}} + \frac{1}{\tau_{capt}} \quad (2.6.15)$$

$$I(t) = I(0) \exp\left(\frac{-t}{\tau_{PL}}\right)^\beta \quad (2.6.16)$$

τ_{PL} in this context is then commonly called decay time. Thus the capture rates can be extracted from PL transients if either the radiative recombination rate is known or at least much smaller than the capture rate. However it is not possible to distinguish between the influences of electron and hole capture [30]. According to the second equation in (2.6.16) the total capture rate is unaffected by exchanging electron and hole relaxation

times and the faster of the two processes will determine the total capture rate [31]. where $I(t)$ is the photoluminescence intensity at time t , I_o is the background intensity level τ_{PL} is $\frac{1}{e}$ decay lifetime, β is the stretch parameter ranges between 0 and 1, and is inversely related to the variance of the decay rate [32].

Chapter 3

Methodology

The study is devoted to the theoretical study and numerical analysis of the On Photoluminescence intensity from GaAs nanostructure with an optical and electrical parameters those affect the photoluminescence intensity that can probe the internal properties of semiconductor nanostructure that those have direct technological contribution can be analyzed with mathematical description of different parameters those supposed were analyzed in simulation with Matlab and fortran code 90 to reach with an arguments that was previously established theoretically and experimentally.

The data we used in this simulation depends on material properties of semiconductor nanostructure and based on experimental works those had been preformed with other scholars. The necessary to employ different codes such as Matlab and fortran 90 .

The apparatus that can be applied to carry out the theoretical part of the project are:

the material which we have employed were: I High capacity computer,

II. Flash discs and

III. Software's for simulating the the photoluminescence intensity.

3.1 Analytical method

In this thesis one of the important methods is solving the problem analytically which is the most important input for the numerical computation.

3.2 Numerical method

For determining the most important optical parameter for photoluminescence intensity we follow to compute the analytical results with some computational tools in MatLab and Fortran 90 codes

Chapter 4

Result and discussion

In this chapter we have discussed on the photoluminescence intensity dependence of optical parameters such as temperature, thickness quantum dot, time resolved, size(diameter) and photon energy the parameters that describe the luminescence intensity with model equations that we have in chapter 2 such as (2.6.1, 2.6.3, 2.6.10, 2.6.15, and 2.6.18). analyzed simulation with matlab and fortran 90 simulation and discussed as follows

4.1 PL Intensity vs Temperature

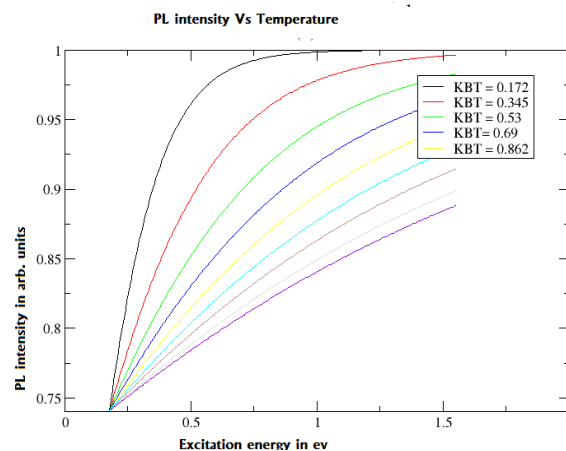


Figure 4.1: PL intensity Vs photon energy matlab simulation result

The data ($T=20k, 40k, 60k, 80k, 100k, 120k, 140k, 160k, 180k$ and $c = 0.035eV$ and $E_a = 0.20eV$) fitting parameters are involved in our

The result of our simulation work also made good agreement with theoretical and experimental values as it shown by figure 4.1 and b Figure 4(1) the emission spectra for a GaAs observed PL intensity increases with low thermal energy.

The activation energy is about 0.20 eV.

Due to the increasing temperature the thermal energy increase at which 1.5 eV PL got quenched then 1.5 eV is quenching thermal energy.

4.2 PL Intensity vs Wavelength

Semiconductors are transparent to photons whose energies lie below their bandgap and are strongly absorbing for photons whose energies exceed the bandgap energy[22]. Then the photoluminescence intensity decreases our simulation shows good argument with supposed theoretical conclusion. As the wavelength increases the PL intensity decreases.

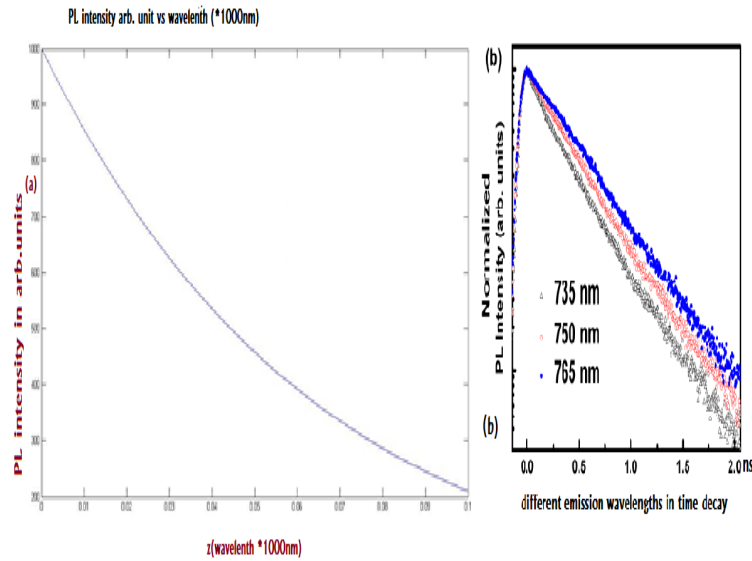


Figure 4.2: PL transient measured at different wavelengths corresponding to the sizes of the GaAs QDs (a) simulation result.(b) taken from reference[19]

4.3 PL Intensity Vs size

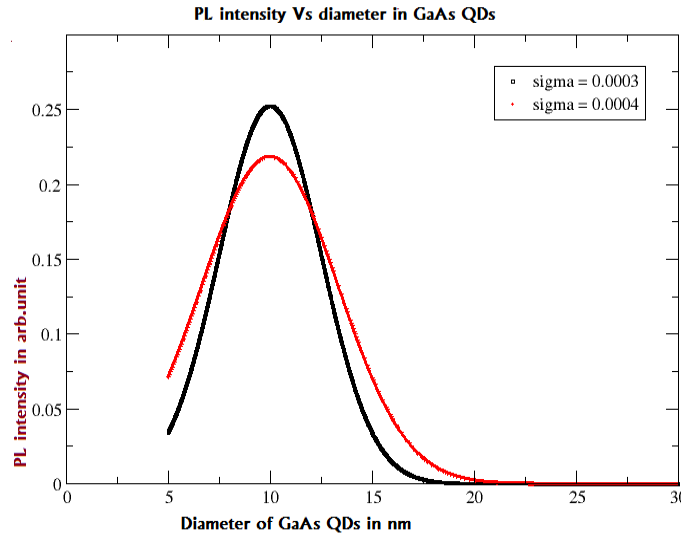


Figure 4.3: PL intensity versus size of the quantum cluster The simulation result when ($\delta = 0.003$ and 0.004)

This result can be explained by a reduction in the exciton oscillator strength in larger dots. A natural choice to find QDs size is to associate the effective size with the diameter of the sphere which has the mass density ρ of bulk GaAs and contains the same number of GaAs clusters as the QD in equation (2.6.15).

From *Eq(3.2.15)* our simulation photoluminescence intensity versus diameter(d) The peak of PL intensity nanocluster structures at mean diameter. The data we took ($d_0 = 10\text{nm}$ and $d = 5\text{nm}$ to 20nm , $\delta = 0.003$ and 0.004). We observed by changing of distribution of the nanocluster the sharper peak of PL intensity is observed. $\delta = 0.0004$ from our simulation we investigated the PL intensity maximum at mean value diameter of GaAs QD when the variation between the cluster is very low and highly confined nanoclusters is the best quality of GaAs QD This implies PL intensity depends on the confinements of nanoclusters.

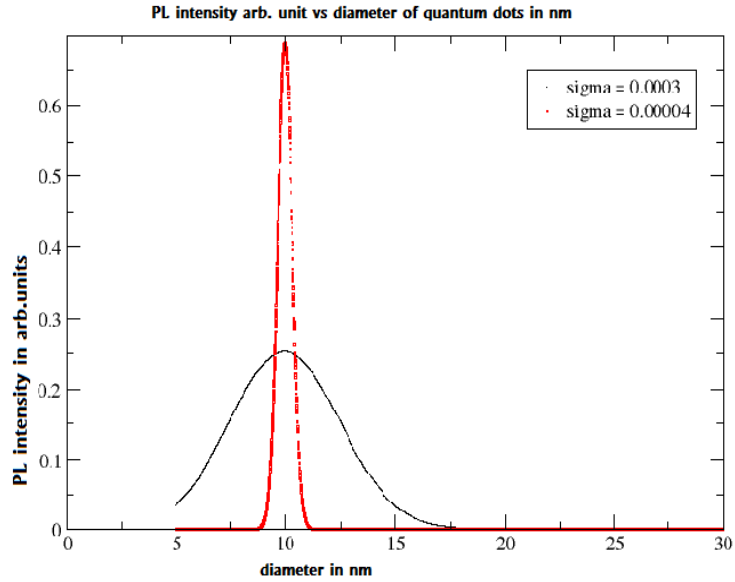


Figure 4.4: PL intensity versus size of the quantum cluster simulation result $\delta = 0.003$ and 0.0004

4.4 PL Intensity Vs Photon energy

This theoretical arguments clearly shown by our simulation which can be observed in figure(4.5.) The photo flux absorbed by semiconductor nanostructures enforce the material's property got to be changed from one phase to other. the excitation of electron- hole changed to tunneling of electron from Valance band to conduction band. For figure (4.5.) the data we have used ($h\nu = 1.5ev, 1.8ev, 2.0ev, 2.2ev, 2.4ev, 2.6ev, 2.8ev, 3.0ev$) thus fitting data in photon energy of visible light wavelength are involved our simulation.

4.5 PL Intensity Vs Time

In time-resolved photoluminescence experiments samples are excited with ultra short light pulses and the change of the emitted light as a function of time is monitored.

From equation (2.6.18)The luminescence decay time is a result of the contributions of

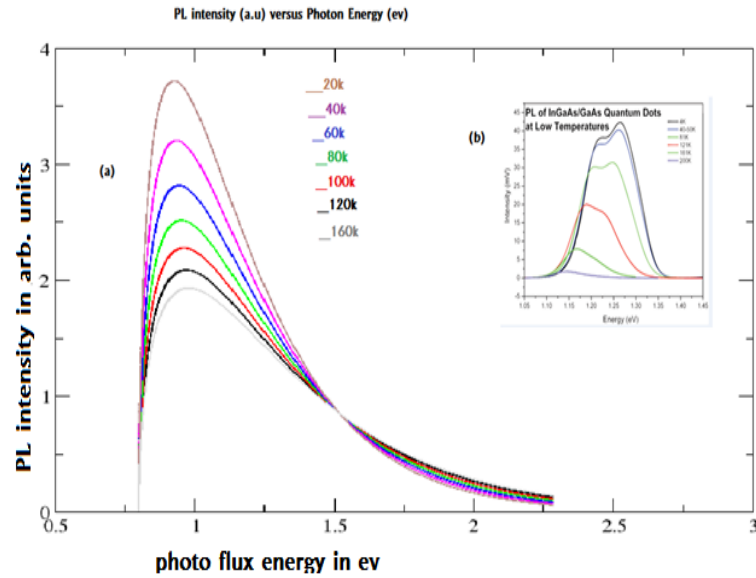


Figure 4.5: PL intensity Vs photon energy (a) simulation result and (b) taken from reference [28]

radiative and non-radiative parts according to the expression[30].

Photoluminescence intensity versus life time depicted in above figure(4.6). As decay life time increases PL intensity decreases. The PL decay time of GaAs QDs increased monotonically with increasing emission wavelength corresponding to the larger dot size due to the reduction of the exciton oscillator strength in the larger dots. The PL decay time of GaAs QDs increased monotonically with increasing emission wavelength corresponding to the larger dot size due to the reduction of the exciton oscillator strength in the larger dots.

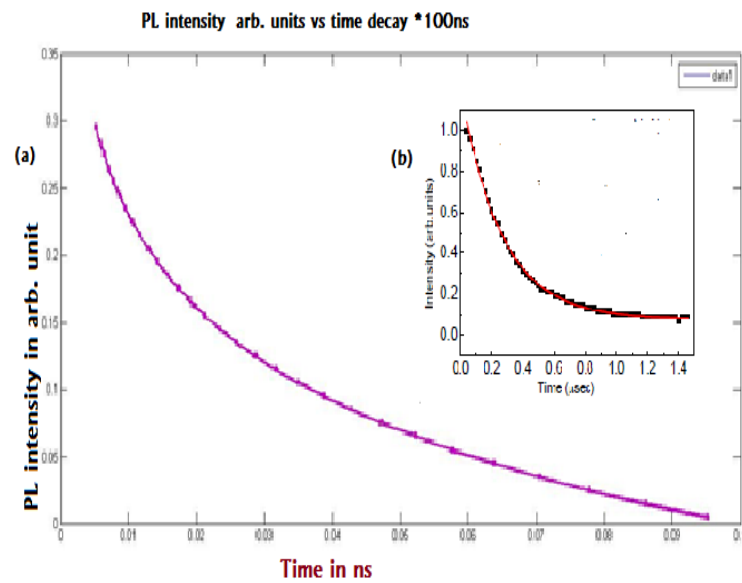


Figure 4.6: PL intensity vs decay time*100ns (a) Diagram that shown the result of matlab simulation and (b) Taken from reference[19]

Chapter 5

Conclusion and future outlooks

5.1 Conclusion

Semiconductor self-assembled QDs demonstrate unique properties related to their similarity to an artificial atoms. They are compatible with standard III-V technology and have no additional defects. These nanostructures have small sizes that yield large confinement energies, and unique properties such as broadband gain/tunability spectra, low chirp, low temperature sensitivity, narrow homogeneous linewidth, and a gain medium robust to material defects [11].

In our simulation model equations of optical parameters those affect the photoluminescence intensity of semiconductors nanostructures do not only inform as the PL intensity but also their chemical and physical properties of materials are probed by this mechanism. The result of our simulation of the model equations argued with theoretical and experimental values.

Temperature-dependent thermal activation of electronic states can be used to estimate their depth below the intrinsic bands. Time-resolved is the PL decay time of GaAs QDs increased monotonically with increasing emission wavelength corresponding to the larger dot size due to the reduction of the exciton oscillator strength in the larger dots [14]

Quantum confinements the semiconductor nanostructures GaAs quantum dots could be found strain free and intrinsic group III-V compound semiconductor GaAs provides the electrical isolation of each device; an important feature in the miniaturization of electronic circuitry.

GaAs is very resistant to radiation damage. with its high efficiency makes GaAs very desirable for outer space applications. All this efficiency of GaAs could studied in mechanism dealing with PL intensity that enable us to informed of semiconductor nanostructure properties, its applications and contribution in technological advancements.

5.2 Future Outlook

The PL signal itself is characterized by three essential features: energy, intensity, and polarization. Because PL is the result of optical transitions between electronic states, the PL spectrum gives precise information on the energy levels available to electrons in the material. The intensity of the PL signal depends on the rate of radiative and nonradiative events, which depends in turn on the density of nonradiative interface states. Therefore I will take to deal with an application of PL on characterization of material properties those have their own contribution for technological applications.

Bibliography

- [1] Timothy H. Gfroerer, *Photoluminescence in Analysis of Surfaces and Interfaces* , John Wiley and Sons Ltd, Chichester, (2000), 9209-9231
- [2] Lingmin Kong, Zhe Chuan Feng,Zhengyun Wu, and Weijie Lu , *Temperature dependent and time-resolved photoluminescence studies of InAs self-assembled quantum dots with InGaAs strain reducing layer structure* , Journal Of Applied Physics , (2009), **106**, 01351
- [3] Jin Z. Zhang and Christian D. Grant, *optical and dynamic properties of undoped and doped semiconductor nanostructures* , Journal of applied physics , University of California, Santa Cruz, CA 95064 USA
- [4] Adachi, s., *Semiconductor cluslors, nanocrystals and quantum dots science* , Nano letters , (1996), **27**(5251), 933
- [5] Pan,H and Y.P.Feng , *Semiconductor nanowire and nanotubes: effects of size and surface to the volume ratio* , journal of applied physics, (2008),**2**(11),2410-2414
- [6] Jingbo Li and Lin-Wang Wang , *Band-structure-corrected local density approximation study of semiconductor quantum dots and wires* , Computational Research Division, Lawrence Berkeley National Laboratory,California 94720, USA ,(2005)
- [7] Hoon Ryu, Dukyun Nam, Bu Young Ahn, JongSuk Ruth Lee, Kumwon Cho, Sunhee Lee, Gerhard Klimeck, Mincheol Shin , *Optical TCAD on the Net: A tight-binding study of inter band light transitions in self-assembled InAs/GaAs quantum dot photodetectors*, Network for Computational Nanotechnology, Purdue University, West Lafayette, IN 47907, USA , (2013), **58**, 288-299

- [8] J. S. Blakemore , *Semiconducting and other major properties of gallium arsenide* publisher= American Institute of Physics , (1982)
- [9] Luf, Wd. and C.M. Lieber , *Lieber, Nano electronic from the bottom up. Nature materials* , Nano letters , (2007),**6** (11),933841-850
- [10] Nader Ghobadi , *Band gap determination using absorption spectrum fitting procedure* International Nano Letters , (2013),**3**(2)
- [11] Richard J. Warburton , *Self-assembled semiconductor quantum dots* Contemporary Physics The University of Leeds, UK , (2002), **43**(5), 351-364
- [12] Shilipi Gupta and Edo Wakes , *spontaneous emission enhancements and Saturable absorption of colloidal quantum dots coupled to photonic crystal cavity* Royal Institute of Technology Department of Microelectronics and Information Technology, Marland.20742 USA
- [13] Fafard, K. Hinzer , and C. N. Allen, *Semiconductor Quantum Dot Nanostructures and their Roles in the Future of Photonics* , Brazilian Journal of Physics, (2004),**34**(2B)
- [14] Jong Su, Kim, *Size Dependence of the Photoluminescence Decay Time in Unstrained GaAs Quantum Dots* , Journal of the Korean Physical Society,(2009)
- [15] Hyun Young Choi, Min Young Cho, Min Su Kim and JaeYoung Leem , *Effects of Rapid Thermal Annealing on the Optical Properties of GaAs Quantum Dots Grown by Using the Droplet Epitaxy Method* Journal of the Korean Physical Society , Korea , (2011),**58**(5), 1324-1329
- [16] Calarco, R., etal, *size-dependent photo conductivity in MBE-Grown GaN-Nanowires* , Nano letters , (2005), **5**(5)
- [17] Debasis Bera, Lei Qian, Teng-Kuan Tseng and Paul H. Holloway , *Quantum Dots and Their Multimodal Applications: A Review* , A Review Materials , (2010),**3**,2260-2345

- [18] G. Huang, F. Xiu, L. He, X. Kou, X. Yu and K. L. Wang. , *Selectively grown III-V Compound Semiconductor Nano/Micro Structures on Silicon for Optoelectronics Applications*, Research Laboratory, Electrical Engineering Department, University of California , Los Angeles, CA 90095,USA,(2011)
- [19] Simpkins, BS., etal, *surface depletion effects in semi conducting nano wires* , journal of applied physics , (2008), **103** 104313-6
- [20] Jongbum Nah, *Thermal Activation of Carriers in InGaAs/InAs/GaAs Quantum Dots* , Journal of the Korean Physical Society, (2009), **54** (1), 127-130
- [21] Bahaa E. A. Saleh, Malvin Carl Teich , *PHOTONS IN SEMICONDUCTORS*, John Wiley and Sons, Inc , (1991)
- [22] K. L. Teo, J. S. Colton, and P. Y. Yu, *An analysis of temperature dependent photoluminescence line shapes in InGaN*, Applied Physics Letters , USA , (1998), **73**(12)
- [23] C.Kittel 8th ed , *Introduction to Solid State Physics, eighth ed* ,John Wiely and Sons, USA, (2005) .
- [24] ZHOU Xiao Hao, CHEN Ping Ping, CHEN Xiao Shuang, LU Wei , *Temperature-Dependent Optical Properties of InAs/GaAs Self Assembled Quantum Dots: Spectroscopic Measurements and an Eight-Band Study* , CHIN. PHYS. LETT , Shanghai 200083 ,(2011), **28**, (11), ,117301
- [25] J. H. Jung, H. C. Im, J. H. Kim, T. W. Kim and K. D Kwack , *Optical Properties and Electronic Structures in InAs/GaAs Quantum Dots.*, Journal of the Korean Physical Society , (2004),**45**, S622-S625
- [26] Adam M. Gilmore. , *Photoluminescence Instrumentation for Nanophotonics Applications*, HORIBA JobinYvon Inc., Fluorescence Division, 3880 Park Ave , address= Edison, NJ 08822 , (2004),6195
- [27] Jrg Siegert, *Semiconductor Quantum Dots Studied by Time-Resolved Photoluminescence Techniques* , Royal Institute of Technology Department of Microelectronics and Information Technology, Optics Section Electrum, San Jose, California,

- [28] S. M. Sze and Kwok K. Ng, *Physics of Semiconductor Devices 3rd edition* A JOHN WILEY and SONS, JNC, San Jose, California, (2007), **3** (2), 602-607
- [29] O. I. Micic, H. M. Cheong, H. Fu, A. Zunger, J. R. Sprague, A. Mascarenhas, and A. J. Nozik, *Size-Dependent Spectroscopy of InP Quantum Dots*, National Renewable Energy Laboratory, 1617 Cole Boulevard, Colorado 8040, (1997), **101**, 4904-4912
- [30] D. Ghodsi Nahri, H. Arabshahi and M. Rezaee Rokn-Abadi, *Analysis of Dynamic and Static Characteristics OF InGaAs/GaAs Self assembled quantum dot lasers*, Armenian Journal of Physics, (2010)
- [31] P. D. Buckle, P. Dawson S. A. Hall, and X. Chen, *Photoluminescence decay time measurements from self-organized InAs/GaAs quantum dots*, Applied Physics Letters, USA, (1999), **86** (12)
- [32] M. Ardyanian and S.A. Ketabi, *Time-Resolved Photoluminescence and Photo-voltaics*, National Renewable Energy Laboratory (NREL), The University of Leeds, UK, (2011), **11**(3)

DECLARATION

I hereby declare that this thesis is my original work and has not been presented for a degree in any other University. All sources of material used for the thesis have been duly acknowledged.

Alemu Gurmessa
email: alemugurmessa@yahoo.com

This thesis has been submitted for examination with my approval as University advisor.

Dr.Pro L.V Choudary

Jimma University